DOI: 10.31534/engmod.2020.3-4.ri.01f
Original scientific paper
Received: 12.06.2020.

Structural integrity of diesel generator set subjected to dynamic loads

Ivo Senjanović, Nikola Vladimir, Damjan Čakmak

University of Zagreb, Faculty of Mechanical Engineering and Naval Architecture, Ivana Lučića 5, 10 000 Zagreb, CROATIA
e-mail: ivo.senjanovic@fsb.hr

SUMMARY

The integrity of the diesel generator set (genset) in the emergency power plant of a Nuclear Power Plant is considered. The genset consists of the diesel engine, the generator, and the common base frame on elastic spring-damper elements clamped to foundations. The genset is exposed to the seismic load, the short circuit impulse, and the synchronization failure load. The problem is solved via the finite element method (FEM). In the FE model, the diesel engine and the generator are represented with two lumped masses rigidly connected to the base frame with sets of massless bars. Strength criteria are specified according to the Russian Federal Codes and Standards in the Area of Atomic Energy Applications. The necessary number of spring-damper elements for preserving the integrity of the genset is determined.

KEY WORDS: *nuclear power plant; diesel generator set; common base frame; elastic springs; seismic load; FEM.*

1. INTRODUCTION

In nuclear power plants, diesel generator sets (gensets) are used in the emergency power plant. A genset consists of a diesel engine, generator, and common base frame placed on elastic supports. A genset is exposed to dynamic loads caused by an earthquake, short circuit, synchronization failure as well as unbalanced diesel engine internal forces. The dynamic response is analyzed with respect to genset static deflection due to its weight.

In this paper evaluation of genset structural integrity is illustrated in the case of ADRIA 40 diesel engine and KONČAR generator. The common base frame is designed and the GERB spring-damper elements are used. The design seismic load is specified for the Bangladesh area. The 2-phase short circuit impulse and the synchronization failure load given by the generator manufacturer are taken into account.

Genset dynamic analysis is performed via the finite element method (FEM) [1]. For this purpose, a FE model is created. The base frame is modelled with shell elements. Assuming that structural integrities of diesel engine and generator are very high, these energetic components are represented by the lumped masses connected to the base frame with sets of stiff bars. The

genset natural vibrations are analysed. The dynamic response of genset is determined for given loads in time domain by means of commercial software.

Strength criteria and capacity of the base frame and the necessary number of spring-damper elements are determined according to the Codes of Russian authorities for nuclear power plants.

2. DIESEL ENGINE AND GENERATOR PARTICULARS

The diesel engine is ADRIA 40+SB 2245-10 with 12 cylinders. The nominal power of the engine is *6600 kW* and the rated speed is 600 RPM. The generator nominal power is *7900 kVA* with *10.5 kV* and *50 Hz*. The genset is shown in Figure 1.

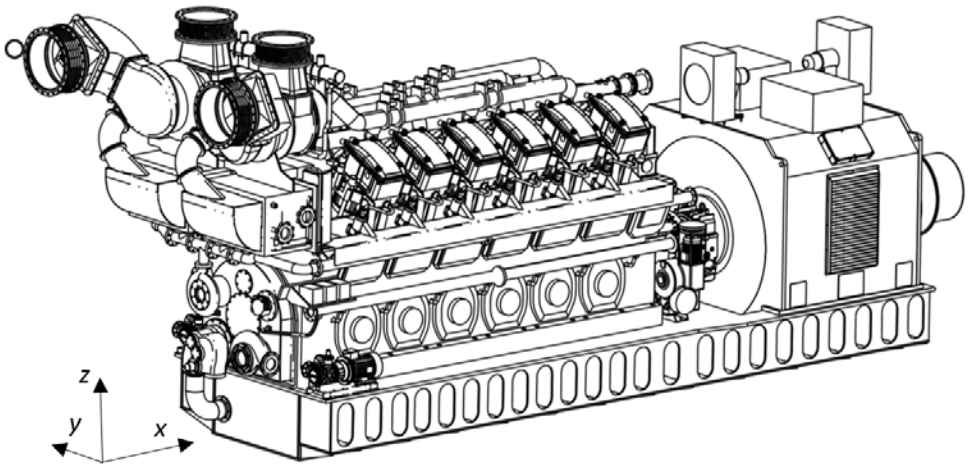

Fig. 1 *Diesel engine and generator on the common base frame*

As mentioned in the Introduction, it is assumed that the strength requirements for both diesel engine and generator are satisfied with respect to prescribed loadings. Therefore, in the generated FE model, they are represented by lumped masses rigidly connected to the base frame with sets of massless bars. The engine and the generator mass moment of inertia with respect to their centres of gravity are determined approximately by assuming homogeneous mass distribution per volume. The following formulas are used:

$$J_x = \frac{M}{12}\left(b^2 + c^2\right), \quad J_y = \frac{M}{12}\left(a^2 + c^2\right), \quad J_z = \frac{M}{12}\left(a^2 + b^2\right), \tag{1}$$

where M is mass, while a, b and c are the engine and the generator length, breadth, and height. The corresponding values for the engine and the generator parameters read:

Engine:

$$M = 82\ t,\ a = 6\ m,\ b = 3\ m,\ c = 3\ m$$

$$J_x = 123\ tm^2,\ J_y = 308\ tm^2,\ J_z = 308\ tm^2$$

Generator:

$$M = 46\ t,\ a = 2.3\ m,\ b = 3\ m,\ c = 1{,}5\ m$$

$$J_x = 43\ tm^2,\ J_y = 30\ tm^2,\ J_z = 55\ tm^2$$

3. BASE FRAME STRUCTURE

The base frame is designed in accordance with the engine and the generator particulars and necessary room for elastic springs, Figure 1. The base frame dimensions are shown in Figure 2. The CAD system is used to get insight into the base frame topology, Figure 3.

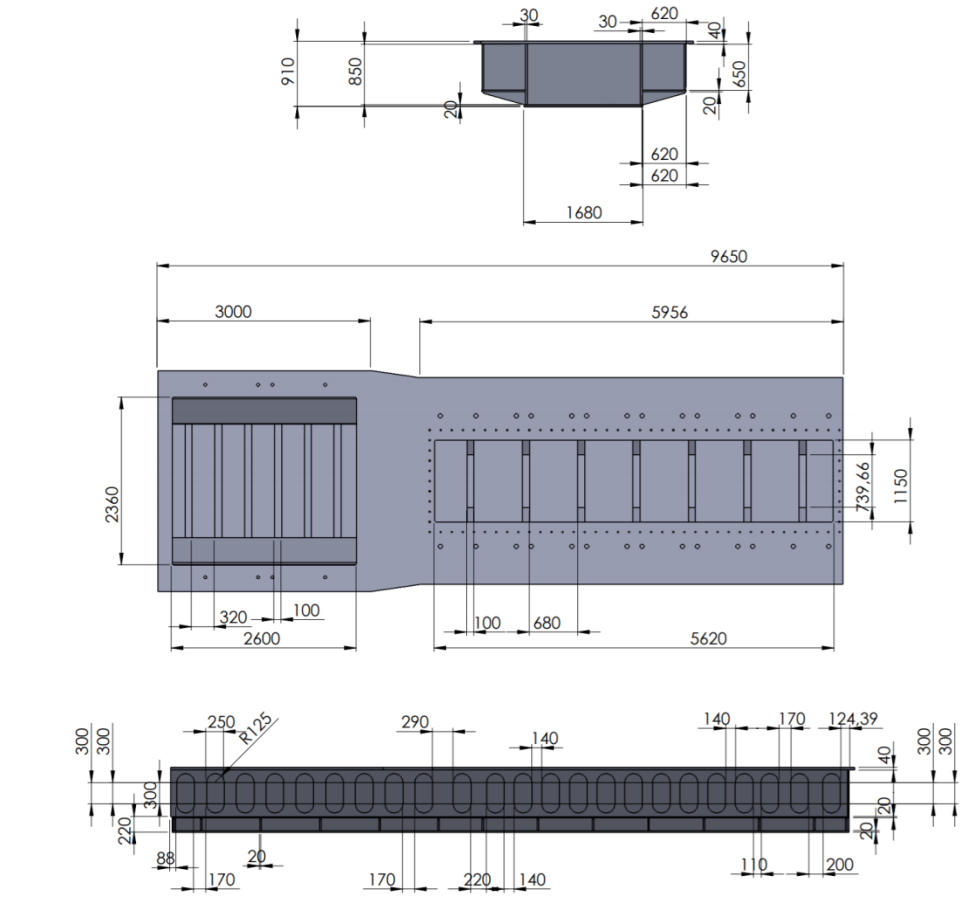

Fig. 2 *The base frame dimensions*

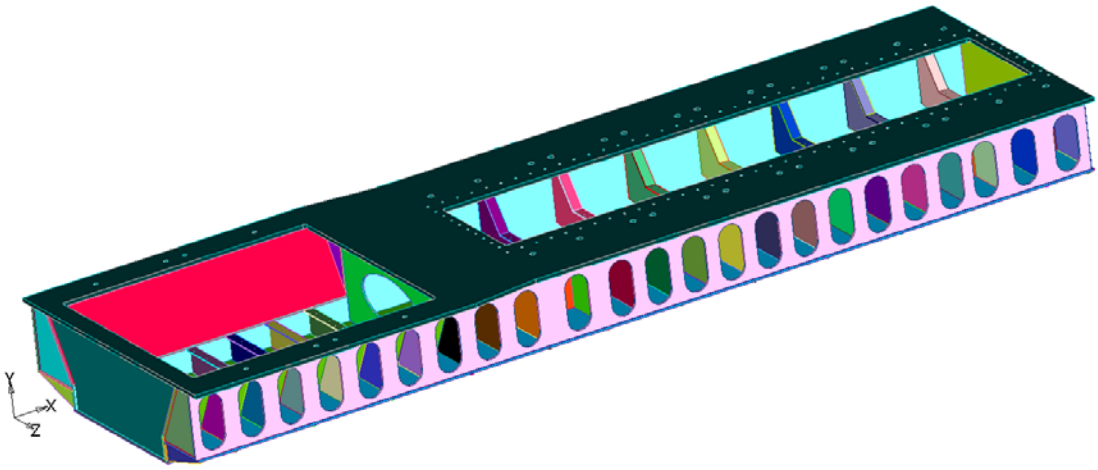

Fig. 3 *The 3D CAD model of the base frame*

The genset schematic presentation is shown in Figure 4 with indicated lumped masses M_G and M_M and their centres of gravity as well as the total center of gravity *CG*. Figure 5 shows the arrangement of *20* spring-damper elements.

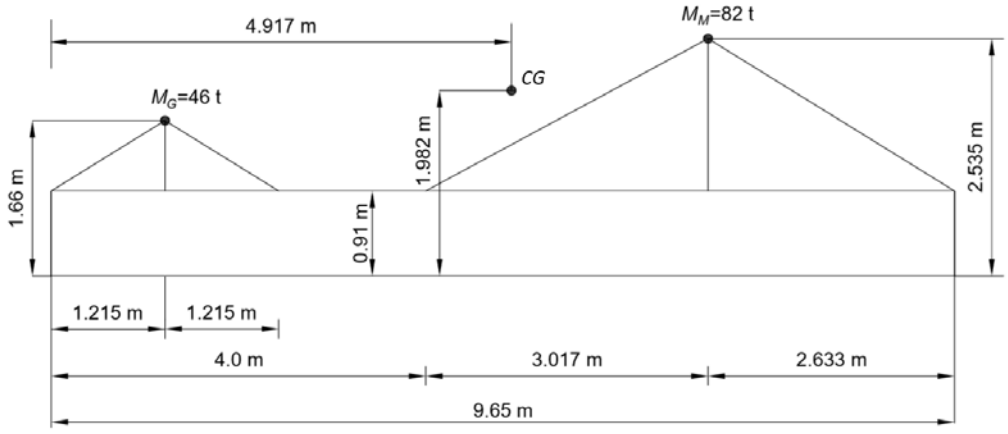

Fig. 4 *The genset schematic representation*

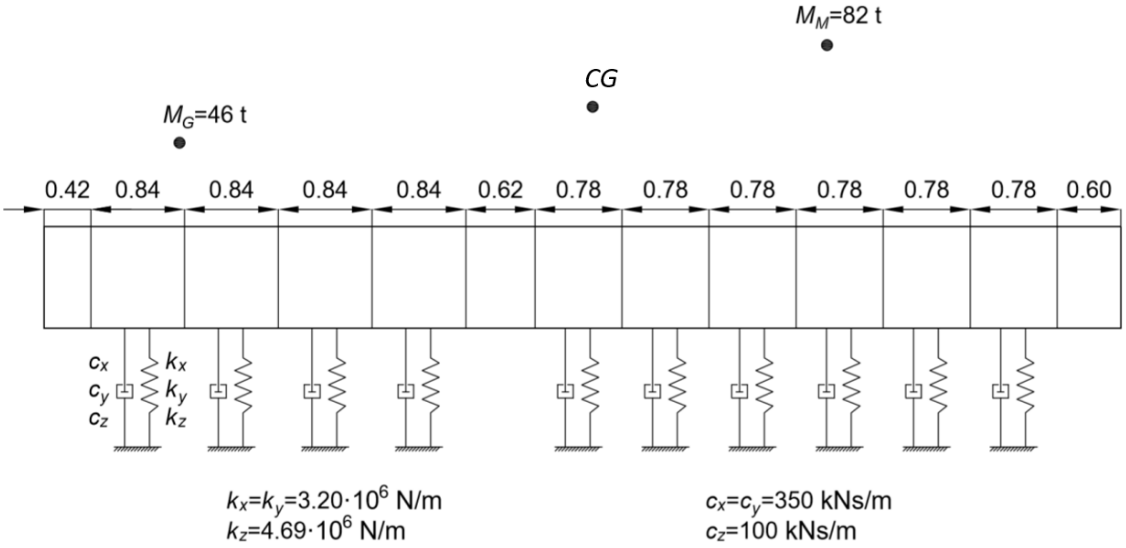

Fig. 5 *The set-up of spring-damper elements*

4. SPRING-DAMPER ELEMENTS

GERB X-10707/20 spring-damper elements are used in this analysis. Their basic particulars are shown in Figure 6. The element vertical and horizontal stiffness and damping coefficients are indicated in Figure 5. The spring-damper elements are connected to the genset base frame and foundation with the adhesive pads shown in Figure 7.

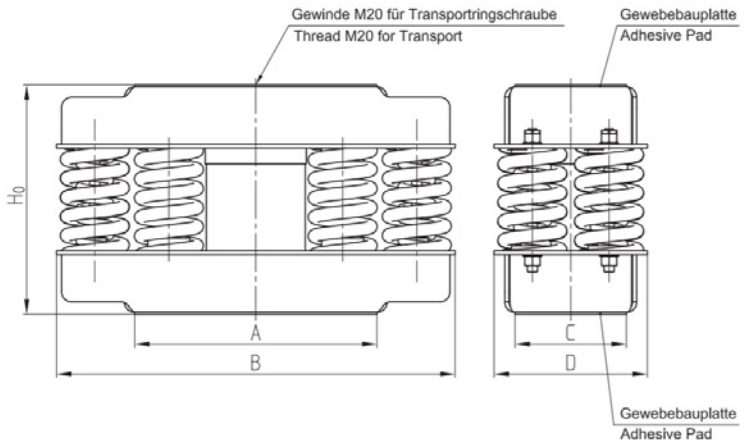

A	B	C	D	H_0
364	635	218	300	448
mm	mm	mm	mm	mm

Fig. 6 *The GERB X-10707/20 spring-damper element*

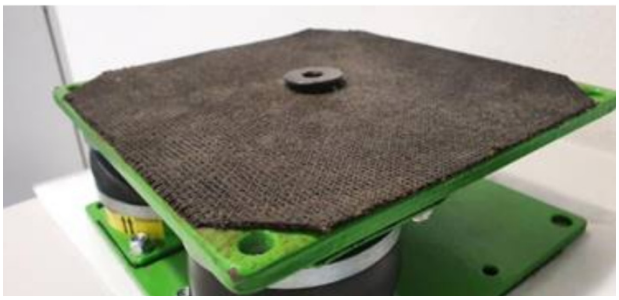

Fig. 7 *The adhesive pad*

The helical spring-damper element includes $n = 8$ active coils made of round wire and incorporated damping device. The exact helical dimensions are not available. Hence, they are estimated according to Figure 6 for purpose of strength analysis:

- wire diameter $d = 25\ mm$,
- mean coil winding diameter $D = 110\ mm$,
- free spring height $H = 200\ mm$.

A vertical force F_z causes torsion in the spring spiral wire. The shear stress is determined by the following formula, [2], [3]:

$$\tau_v = \frac{8F_z D}{n\pi d^3}, \tag{2}$$

where n represents the number of coils in the spring. In a similar way, one can write for shear stress due to horizontal force F_y:

$$\tau_h = \frac{8F_y H}{n\pi d^3}. \tag{3}$$

5. FINITE ELEMENT MODEL OF THE GENSET

Based on the relevant data specified in the previous sections, a 3D FE model of the analysed system is generated by NASTRAN package [4], Figure 8. As stated earlier, the generator and engine are modelled by lumped mass elements rigidly connected to the base frame with two sets of massless bars. The base frame is supported with *20* elastic spring-damper elements, i.e. 10 elements on each side. The upper nodes of spring-damper elements are connected to the base frame, while the lower ones are clamped to the foundation. In total, the finite element model, Figure 8, comprises *21770* elements, i.e. *21746* shell elements, *20* spring-damper elements, two lumped mass elements, and two rigid connecting elements simulating sets of rigid bars (according to NASTRAN notation), and there are *21252* nodes.

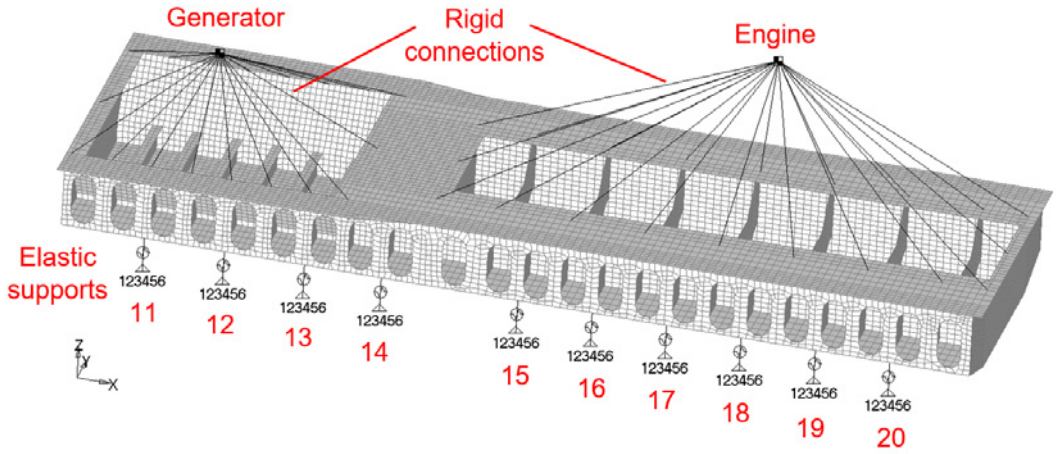

Fig. 8 *The finite element model of the genset*

Mass of the finite element model includes the following items:

– generator mass: $M_G = 46\ t$,

– engine mass: $M_M = 82\ t$,

– base frame mass: $M_F = 20\ t$,

– mass of lubrication oil: $M_O = 6.5\ t$,

Total mass yields *154.5 t*. As pointed out in the previous sections, generator mass and engine mass are specified as lumped masses. Distributed base frame mass and mass of lubrication oil in the base frame are defined by common mass density as:

$$\rho = \rho_{st}\left(1+\frac{M_O}{M_F}\right), \tag{4}$$

where $\rho_{st} = 7.85\ t/m^3$ is the steel mass density.

The following calculations are performed via the above described FE model:

– static analysis due to the gravity load,

– free vibration analysis,

– forced vibration analysis due to the seismic load,

– forced vibration analysis due to the 2-phase short circuit impulse,

– forced vibration analysis due to the synchronization failure load.

Each of the above calculations requires a different calculation setup, as elaborated in the next sections.

6. DESIGN EARTHQUAKE

The seismic building integrity can be checked for a real earthquake and/or building resistance can be estimated by imposing a design earthquake, [5], [6], [7]. The considered nuclear power plant (NPP) is located in Bangladesh. Hence, the earthquake registered in Kathmandu, Nepal on April 25th, 2015 with a magnitude of *7.8 MW* can be used as a relevant one. The three-component accelerogram of this earthquake is shown in Figures 9 – 11. Figure 12 shows the spectrum of total acceleration.

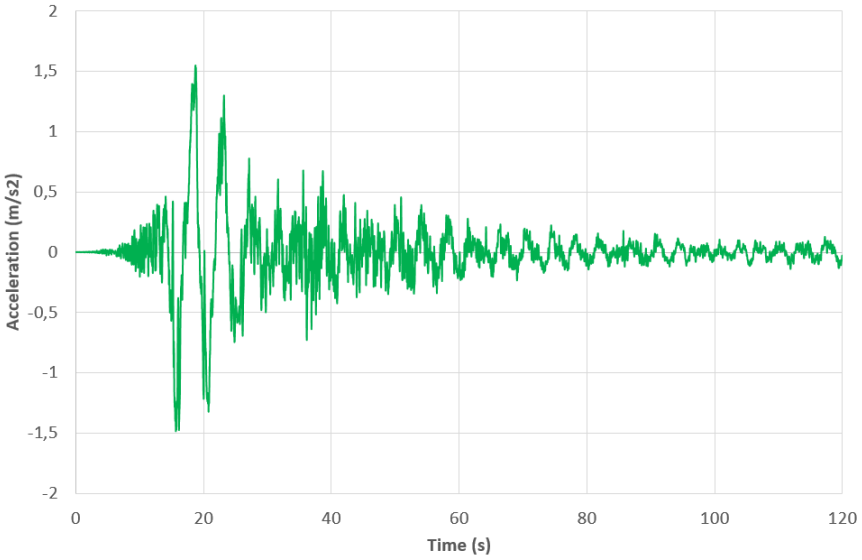

Fig. 9 *Ground acceleration in x-direction recorded during earthquake in Kathmandu on April 25th, 2015*

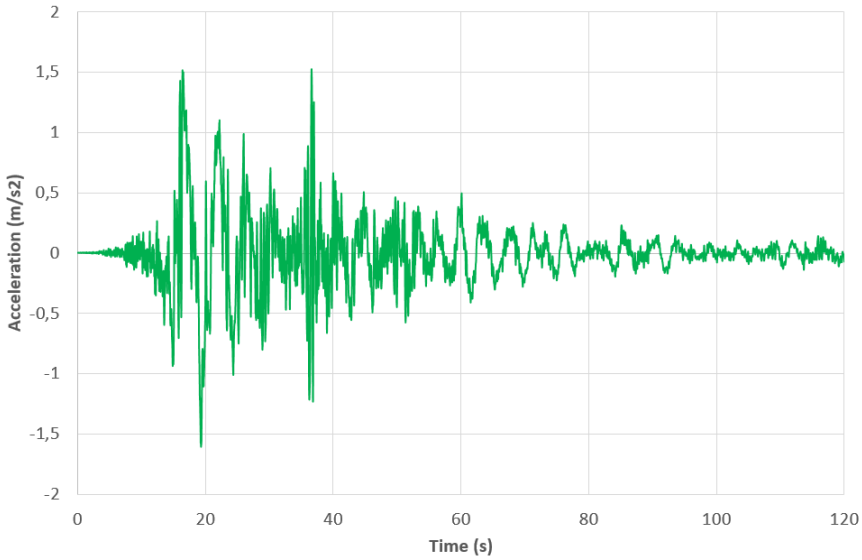

Fig. 10 *Ground acceleration in y-direction recorded during earthquake in Kathmandu on April 25th, 2015*

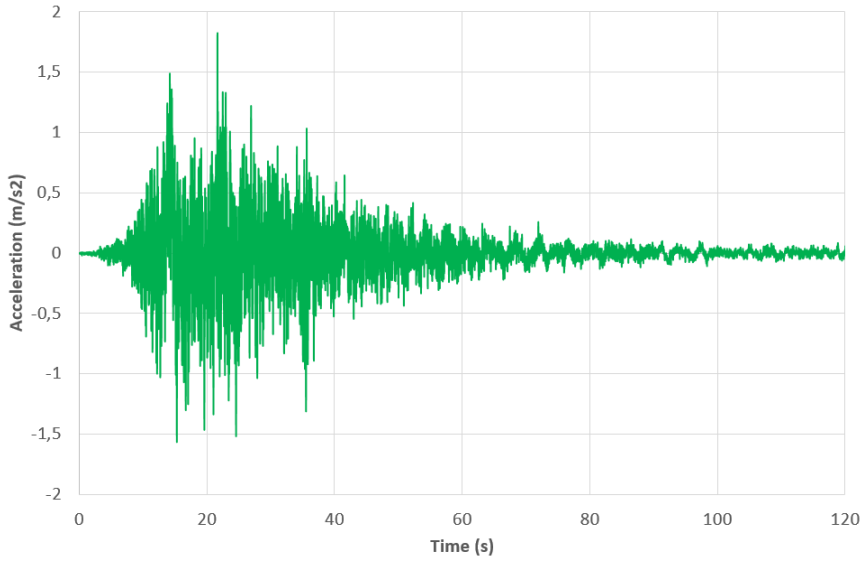

Fig. 11 *Ground acceleration in z-direction recorded during earthquake in Kathmandu on April 25th, 2015*

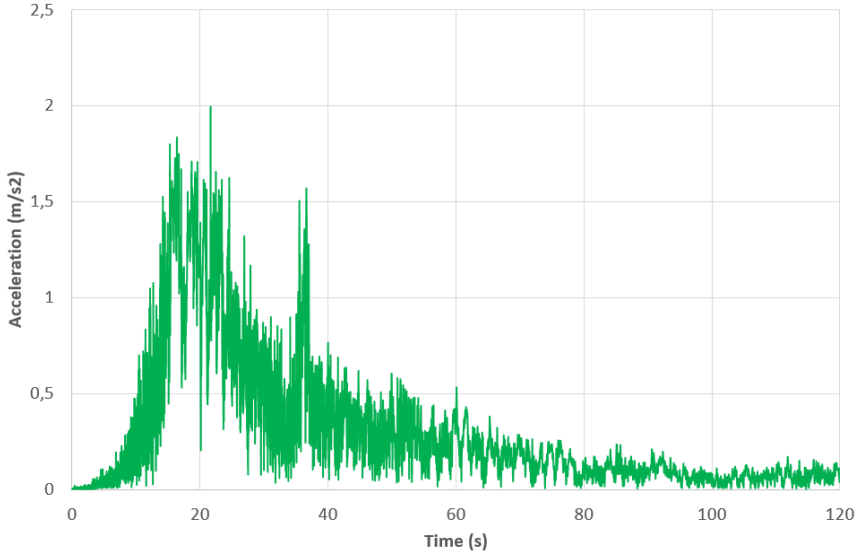

Fig. 12 *Total acceleration spectrum of earthquake in Kathmandu on April 25th, 2015*

The genset is placed on the ground floor of the emergency diesel electric power plant. A design earthquake is defined by following the statistics of real earthquakes. Procedure for estimation of the building safety includes building classification, geotechnical conditions of location, FE model of the building-foundation system, and calculation of its dynamic behaviour by time integration using a commercial FEM package. As a result, diagrams of the acceleration components are obtained. Margins of these components at the ground floor level yield: $A_x = \pm 2.02\ m/s^2$, $A_y = \pm 1.97\ m/s^2$, $A_z = \pm 1.39\ m/s^2$.

In the absence of the digital time record, the acceleration of design earthquake for the ground floor is reconstructed for needs of genset dynamic analysis within the above margins by the following formula:

$$a(t) = C\sum_{i=1}^{n} A_i(\omega_i)\cdot cos(\omega_i t + \varepsilon_i), \tag{5}$$

where $A_i(\omega_i)$ are the spectral acceleration amplitudes taken from the building response spectrum, ω_i are spectral frequencies in the range of *0* to *50 Hz*, ε_i are random phase angles, $n = 65$, and C represents an adaptive factor to ensure margins of design accelerations. Acceleration components for the genset design earthquake are shown in Figures 13 – 15. Figure 16 shows the total acceleration spectrum.

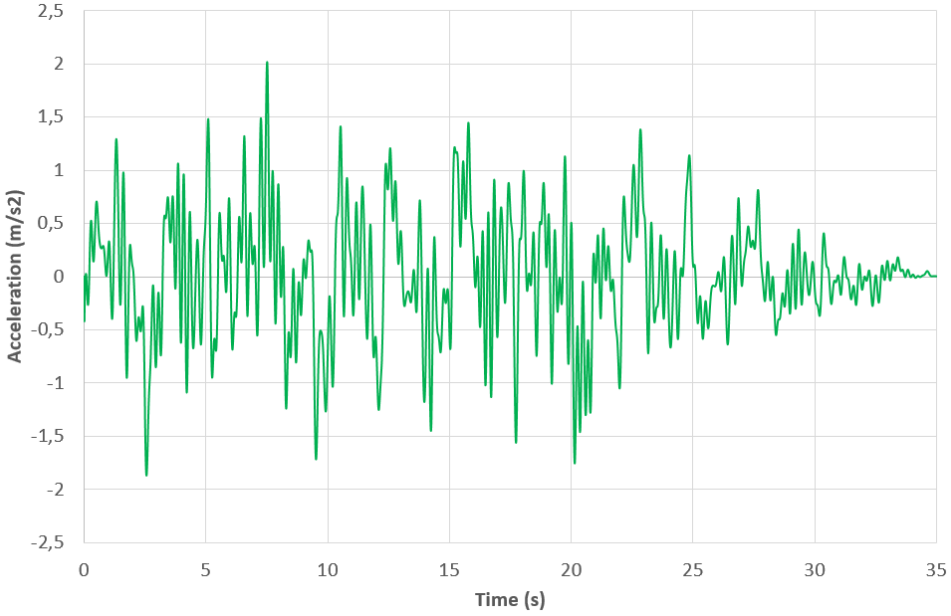

Fig. 13 *Design earthquake acceleration in x-direction*

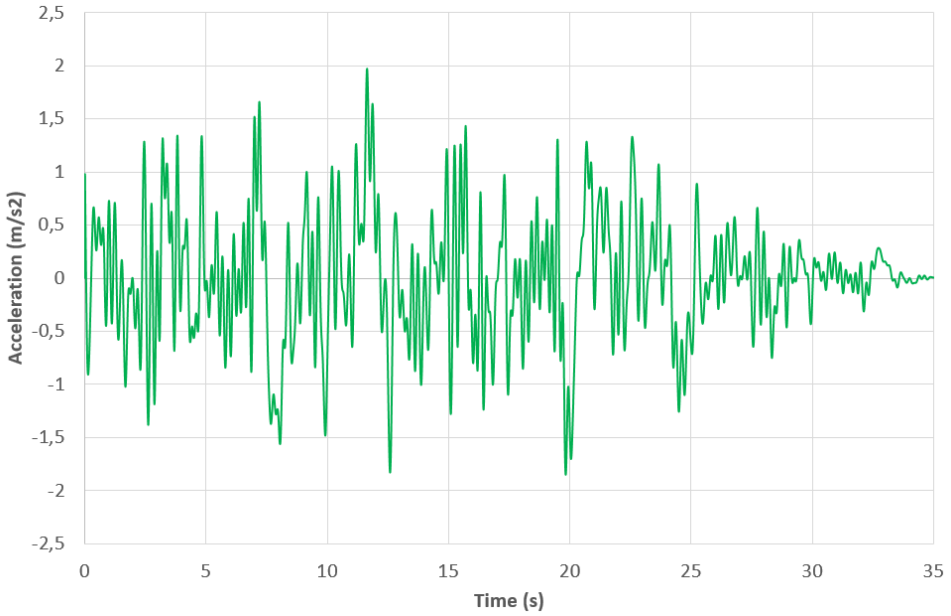

Fig. 14 *Design earthquake acceleration in y-direction*

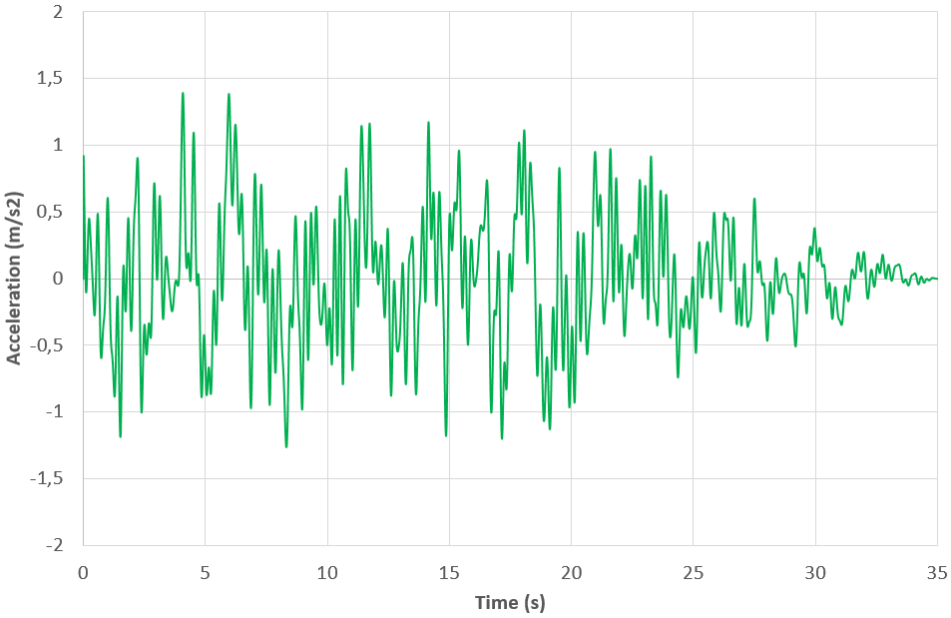

Fig. 15 *Design earthquake acceleration in z-direction*

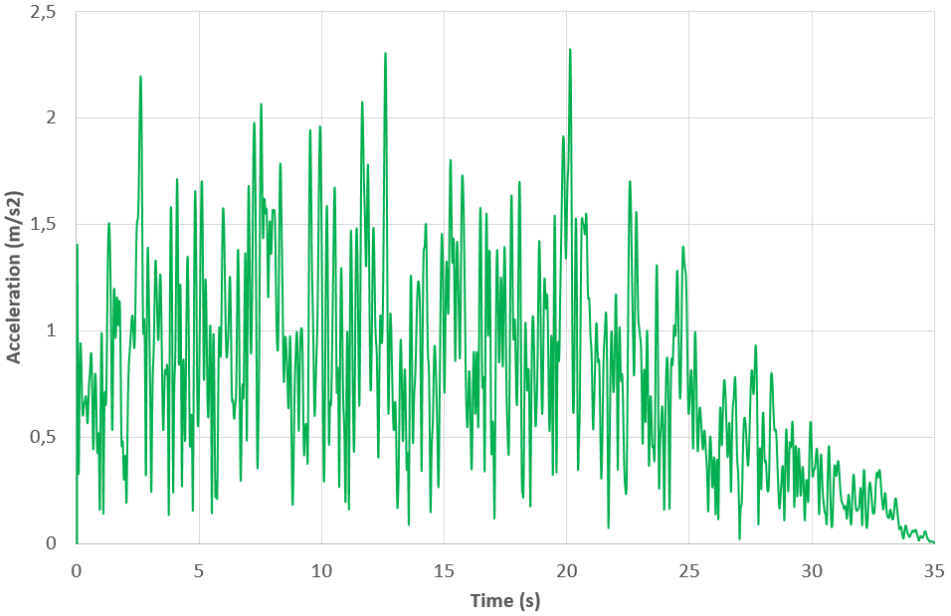

Fig. 16 *Total design earthquake acceleration spectrum*

7. GENSET STATIC ANALYSIS

Static load of genset consists of the following gravity components:

– generator weight: $W_G = 451.26\ kN$,

– engine weight: $W_M = 804.42\ kN$,

– base frame weight: $W_F = 196.20\ kN$,

– weight of lubrication oil: $W_O = 63.76\ kN$.

The total weight of the genset is $W = 1515.64\ kN$.

Von Mises total (membrane and bending) stresses in the base frame structure are shown in Figure 17. The stress concentration occurs at the connection of spring-damper elements to the base frame structure. The peak values are around $40\ MPa$, which is quite low as a result of a large number of almost equidistantly distributed springs. Von Mises membrane stresses are predominant in the total stresses.

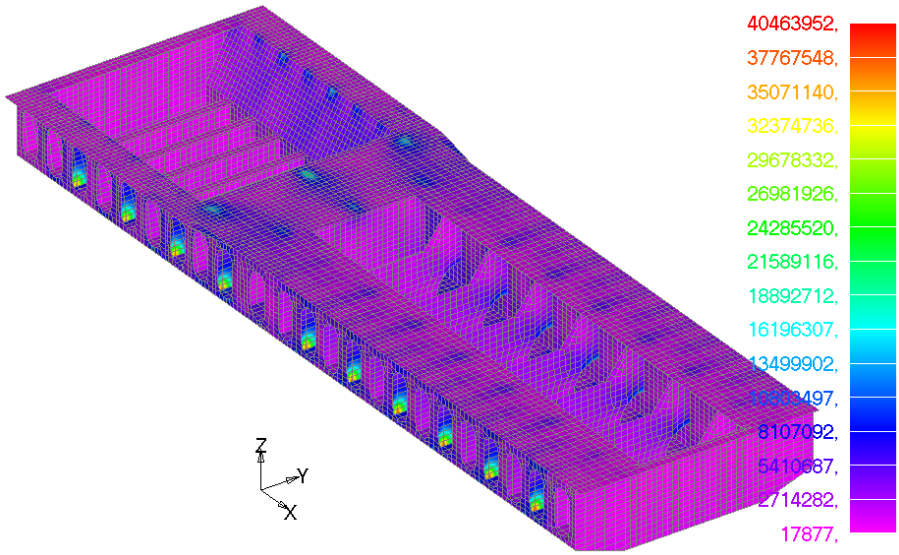

Fig. 17 *Von Mises total stresses in base frame due to gravity load, σ (Pa)*

More interesting are gravity reaction forces in supports, which are presented in Table 1. The reaction forces on the left and right hand side are the same due to the symmetric structure and gravity load. The values of reaction forces are slightly increased from the generator to the engine.

Table 1 *Gravity reaction forces*

Spring No.	*Node No.*	F_z *(kN)*	*Spring No.*	*Node No.*	F_z *(kN)*
1	9208	73.98	11	1371	73.98
2	9215	73.96	12	7905	73.96
3	9462	73.95	13	8719	73.95
4	9519	74.10	14	9157	74.10
5	9389	75.14	15	8708	75.14
6	9216	75.86	16	8018	75.86
7	9217	76.60	17	8194	76.60
8	9213	77.34	18	4077	77.34
9	9388	78.09	19	8195	78.09
10	9209	78.88	20	1373	78.88

Mean value of spring gravity force is $\overline{F}_z = W/n = 75.78\ kN$. Shear stress in spring coil due to average force determined by Eq. (2) takes value $\overline{\tau}_{st} = 170\ MPa$, while the maximum static stress is $\tau_{st} = 177\ MPa$.

8. GENSET NATURAL VIBRATIONS

In the obtained natural frequencies spectrum, values of the first six frequencies are very low since they are related to genset rigid body motion on elastic supports. In Figures 18 – 20, the first three genset elastic natural modes are shown with corresponding natural frequencies. The first mode is of vertical vibrations; the second of torsional vibrations, while the third is a horizontal mode. Their order is a result of vertical, torsional, and horizontal stiffness relationships. In all modes, maximum base frame deformations occur in the area between generator and engine, since these two rigidly connected solid energetic components increase the base frame stiffness in their spans.

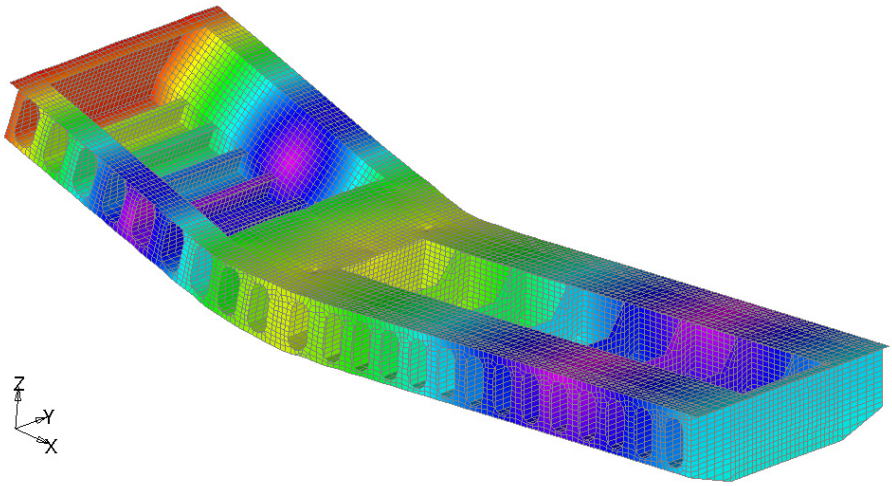

Fig. 18 *The first vertical natural bending mode of base frame, ω_7 = 20.41 Hz*

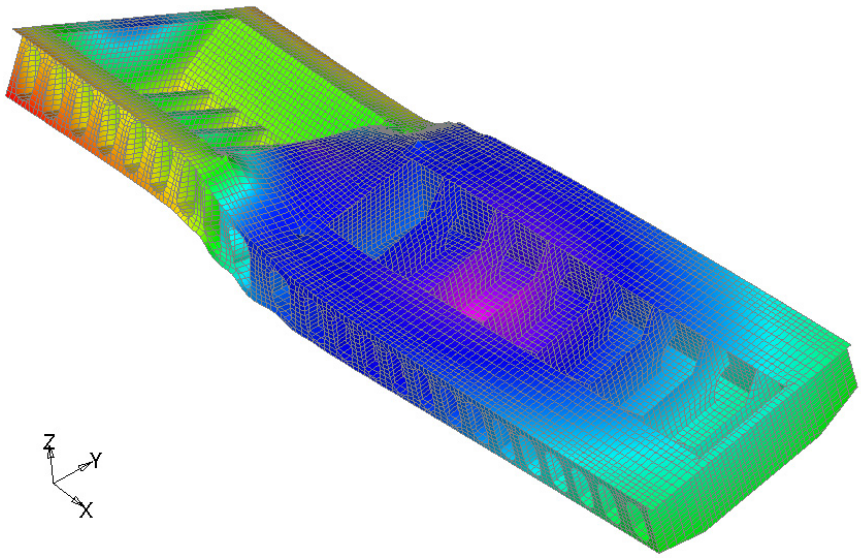

Fig. 19 *The first torsional natural mode of base frame, ω_8 = 35.44 Hz*

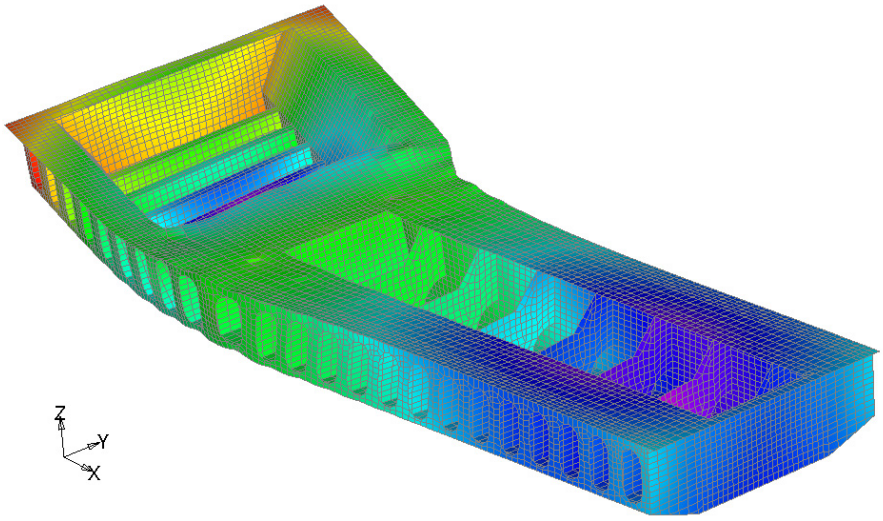

Fig. 20 *The first horizontal natural mode of base frame, ω_9 = 67.40 Hz*

9. GENSET RESPONSE TO DESIGN EARTHQUAKE

In general, matrix differential equations of motion of a dynamic system exposed to ground excitation in the finite element formulation reads, [5], [6], [7]:

$$[M]\{\ddot{\Delta}\}+[C]\left(\{\dot{\Delta}\}-\{\dot{d}\}\right)+[K]\left(\{\Delta\}-\{d\}\right)=\{0\}, \tag{6}$$

where $[M]$ is the mass matrix, $[C]$ is the damping matrix, $[K]$ is the stiffness matrix, $\{\Delta\}$ is the vector of total displacements and $\{d\}$ is the vector of ground displacements.

If ground displacements and velocities are known, Eq. (6) can be written in the form:

$$[M]\{\ddot{\Delta}\}+[C]\{\dot{\Delta}\}+[K]\{\Delta\}=\{F(t)\}, \tag{7}$$

where:

$$\{F(t)\}=[C]\{\dot{d}\}+[K]\{d\}, \tag{8}$$

is the excitation force vector.

In the case of an earthquake, the ground acceleration is recorded, and Eq. (6) is rearranged in the form:

$$[M]\{\ddot{\delta}\}+[C]\{\dot{\delta}\}+[K]\{\delta\}=-[M]\{\ddot{d}\}, \tag{9}$$

where $\{\delta\} = \{\Delta\} - \{d\}$ is the vector of relative structure displacements with respect to the ground motion.

In the case of formulation (7), total displacements $\{\Delta\}$ are obtained directly. However, if Eq. (9) is applied, relation $\{\Delta\} = \{\delta\} + \{d\}$ holds. Hence, both formulations lead to the same results.

The genset response to the design earthquake is determined by NASTRAN package, [4]. The three components of ground acceleration, Figures 13 – 15, are imposed simultaneously to the FE model, Figure 8. The problem is solved in the time domain. For illustration, the time history of reaction forces in spring No. 11 (node 1371) is shown in Figures 21 – 23 due to maximum peaks. In addition, the absolute values of the total reaction force can be seen in Figure 24.

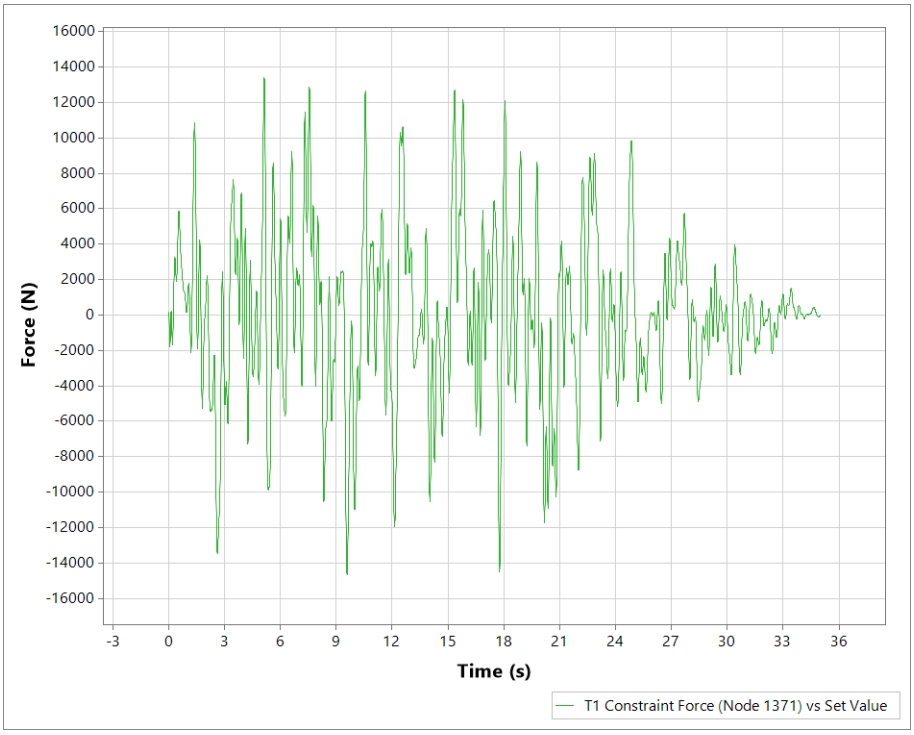

Fig. 21 *Reaction force of spring No. 11 in x-direction due to seismic load*

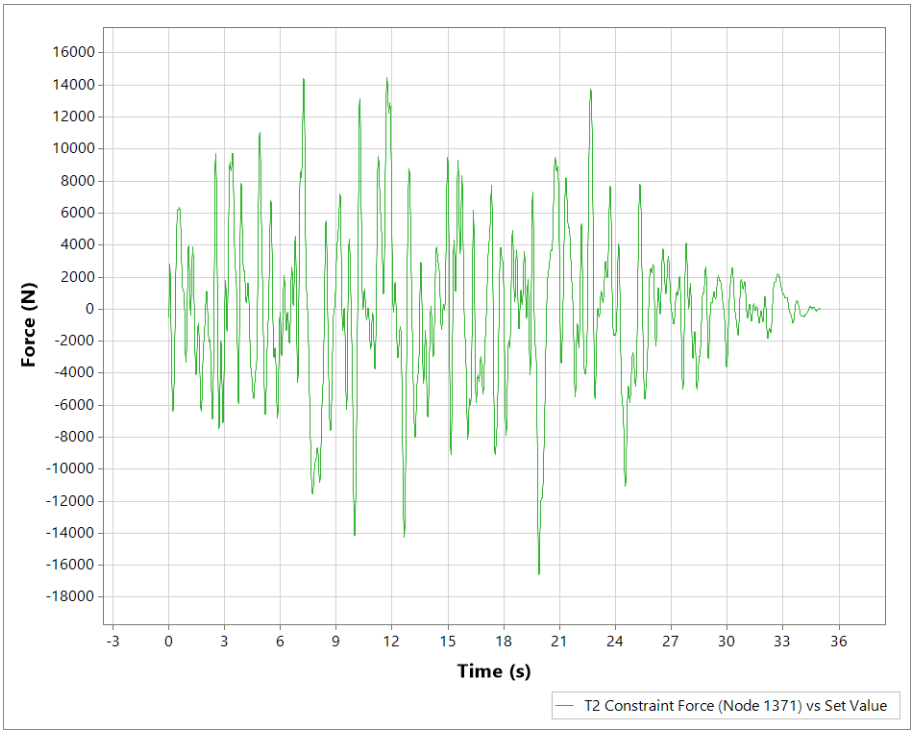

Fig. 22 *Reaction force of spring No. 11 in y-direction due to seismic load*

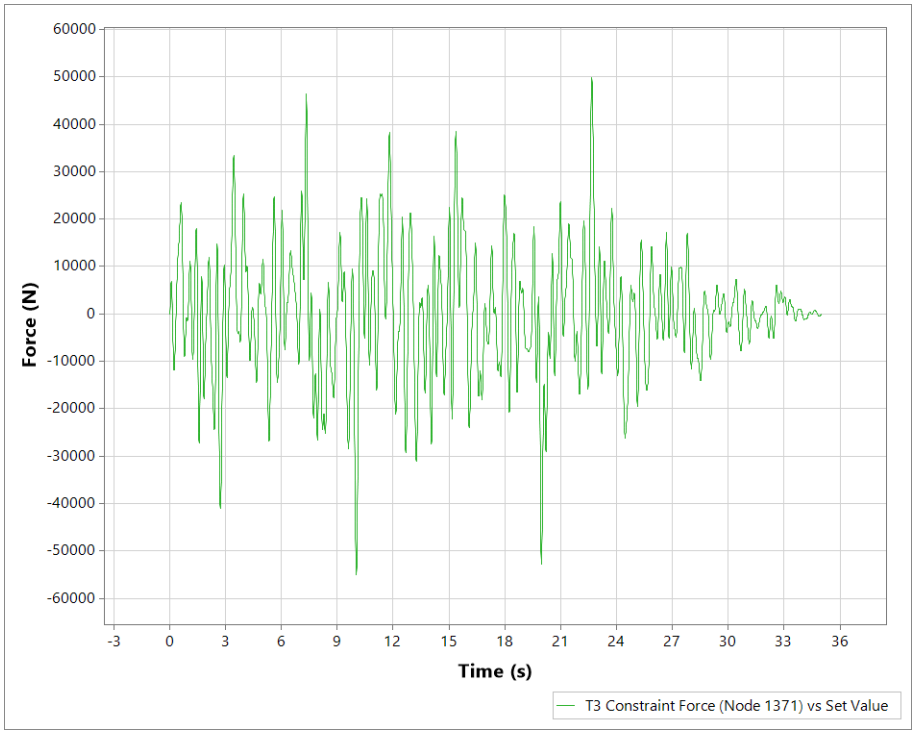

Fig. 23 *Reaction force of spring No. 11 in z-direction due to seismic load*

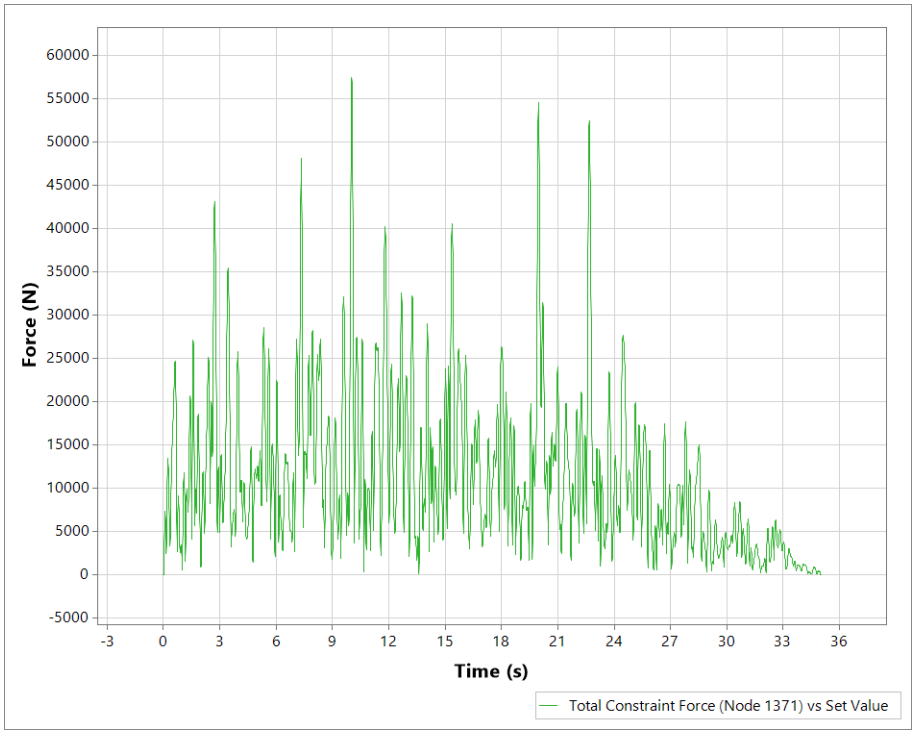

Fig. 24 *Total reaction force of spring No. 11 due to seismic load*

Maximum values of seismic reaction forces, independently on time instant, are shown in Table 2 for all 20 springs. Forces in the right side springs (Nos. 11 – 20) are somewhat larger than

those in the left side springs (Nos. 1 – 10), due to genset rotation around the *x*-axis caused by transverse ground acceleration a_y.

Table 2 *Maximum seismic reaction forces (independent on time instant)*

Spring No.	F_x *(kN)*	F_y *(kN)*	F_z *(kN)*	*F (kN)*
1	*16.65*	*16.59*	*42.50*	*45.23*
2	*16.64*	*16.53*	*39.09*	*41.87*
3	*16.65*	*16.38*	*35.69*	*38.86*
4	*16.67*	*16.56*	*33.99*	*37.14*
5	*16.69*	*17.49*	*32.85*	*36.77*
6	*16.67*	*17.57*	*32.32*	*36.25*
7	*16.67*	*17.71*	*33.22*	*36.24*
8	*16.67*	*17.94*	*35.62*	*40.50*
9	*16.67*	*18.26*	*39.67*	*44.18*
10	*16.68*	*18.75*	*43.74*	*47.97*
11	*14.68*	*16.61*	*55.04*	*57.46*
12	*14.68*	*16.55*	*50.60*	*53.31*
13	*14.68*	*16.41*	*47.29*	*49.63*
14	*14.68*	*16.61*	*45.13*	*47.75*
15	*14.65*	*17.55*	*42.04*	*45.26*
16	*14.63*	*17.64*	*43.48*	*46.33*
17	*14.62*	*17.77*	*44.84*	*47.82*
18	*14.62*	*17.97*	*46.30*	*49.31*
19	*14.62*	*18.25*	*47.98*	*50.82*
20	*14.62*	*17.72*	*49.70*	*52.54*

Shear stresses in the spring coils due to vertical and horizontal forces are determined according to Eqs. (2) and (3) respectively. Four corner springs, i.e. Nos. 1, 10, 11, and 20 as the representative ones, are considered. For this purpose, it is necessary to determine the resulting horizontal force, F_h, at the time instant of the maximum total force, F_t. Since vertical force, F_z, is dominant in total force, Table 2, peak values of these two forces appear at the same time instant. The corresponding horizontal force at that time instant reads:

$$F_h(t_i) = \sqrt{F_t^2(t_i) - F_z^2(t_i)}. \tag{10}$$

The determination of $F_h(t_i)$ is illustrated in Figure 25. Shear stresses in representative springs, calculated by Eqs. (2) and (3), are shown in Table 3.

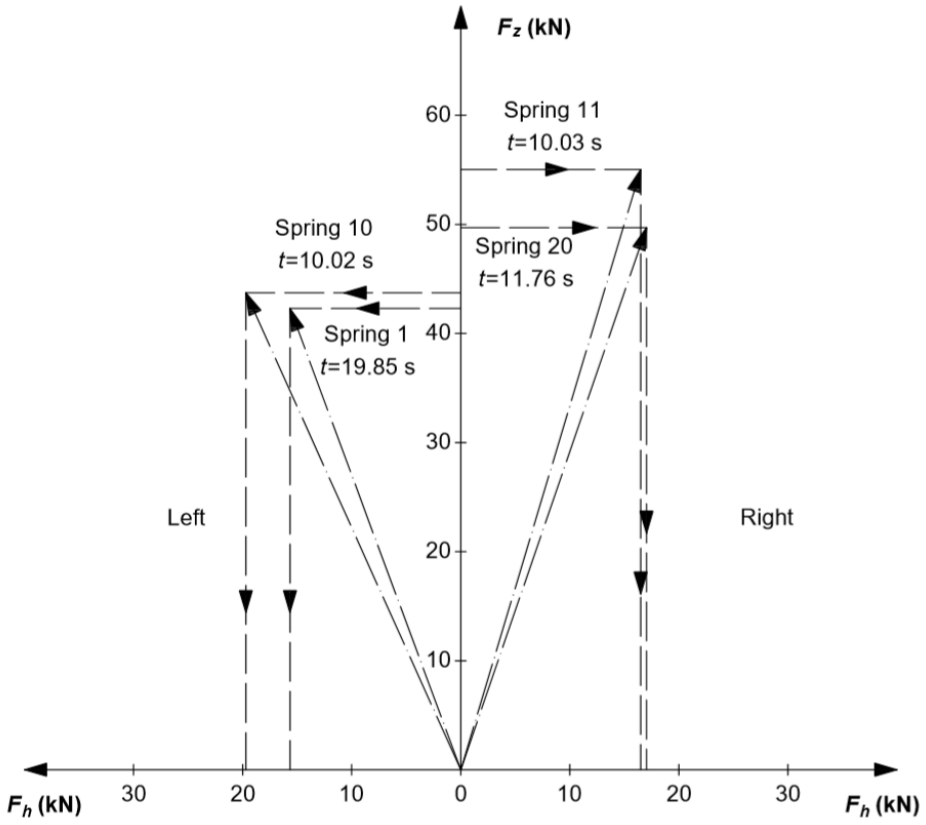

Fig. 25 *Determination of horizontal seismic forces in representative springs*

Table 3 *Maximum seismic shear stresses τ (MPa)*

Spring No.	***Node No.***	τ_{F_z}	τ_{F_h}	τ_{tot}
1	*9208*	*96*	*67*	*163*
10	*9209*	*100*	*79*	*179*
11	*1371*	*127*	*65*	*192*
20	*1373*	*112*	*86*	*198*

Regarding von Mises stresses in the base frame, their largest values appear at the connection of spring elements to the base frame bottom, as can be seen in Figure 26. The maximum stresses reach a value of *85 MPa*. However, this stress concentration is not reliable enough since it is a result of the spring point connection to the base frame plating in the FE model. In reality, the large spring pad area somewhat smoothes the stress concentration, Figure 7. For illustration, the time history of high von Mises stresses in one of the bottom plating finite elements is presented in Figure 27.

In addition, the total acceleration at the generator centre of gravity and the engine centre of gravity are shown in Figures 28 and 29 respectively. In both cases, the acceleration peaks are somewhat higher than the ground acceleration peaks, Figure 16.

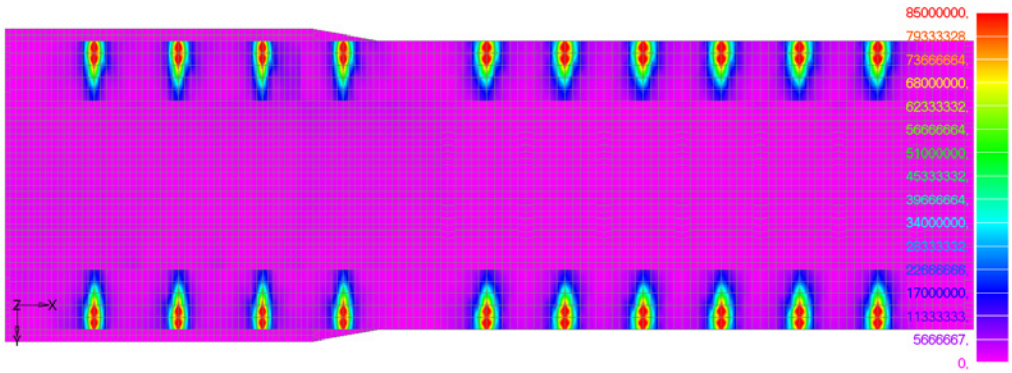

Fig. 26 *Von Mises total seismic stresses in the base frame bottom, t = 10.0 s*

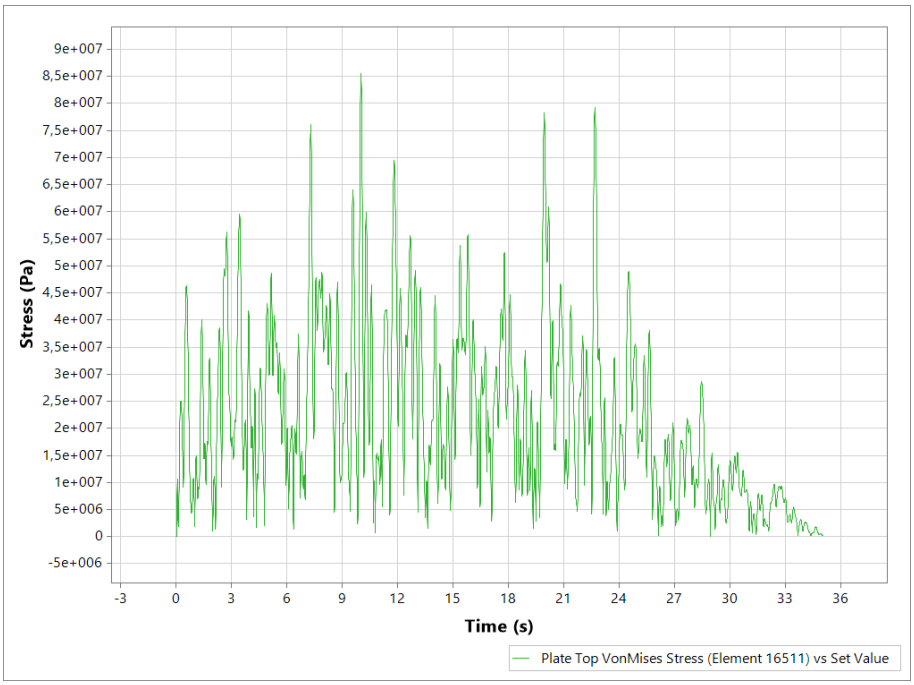

Fig. 27 *Time history of von Mises seismic stresses in the base frame bottom finite element, σ (Pa)*

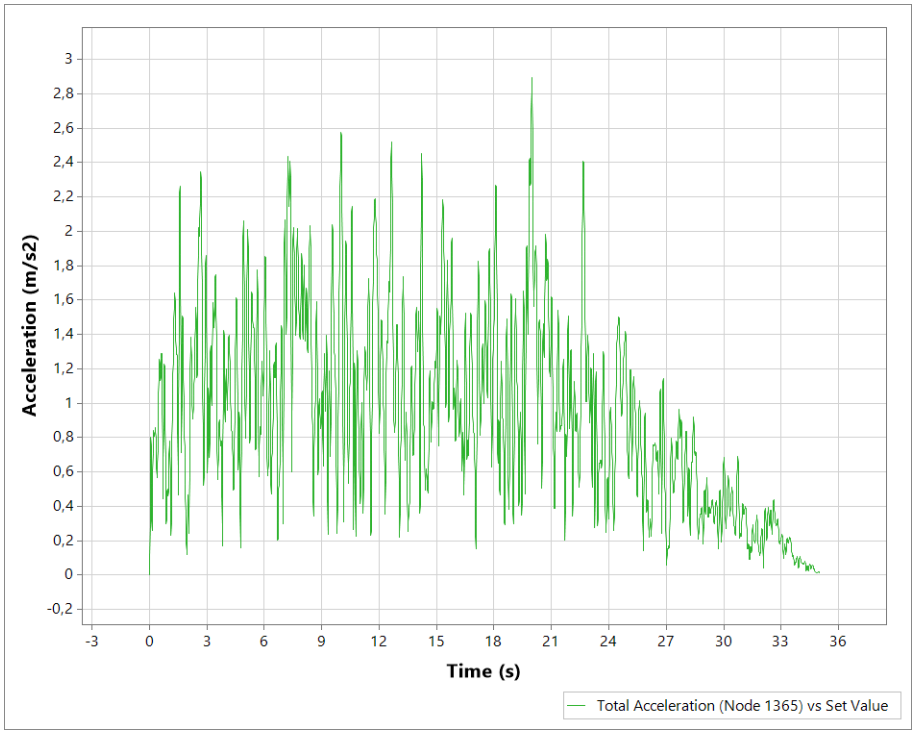

Fig. 28 *Total acceleration of the generator centre of gravity due to seismic load*

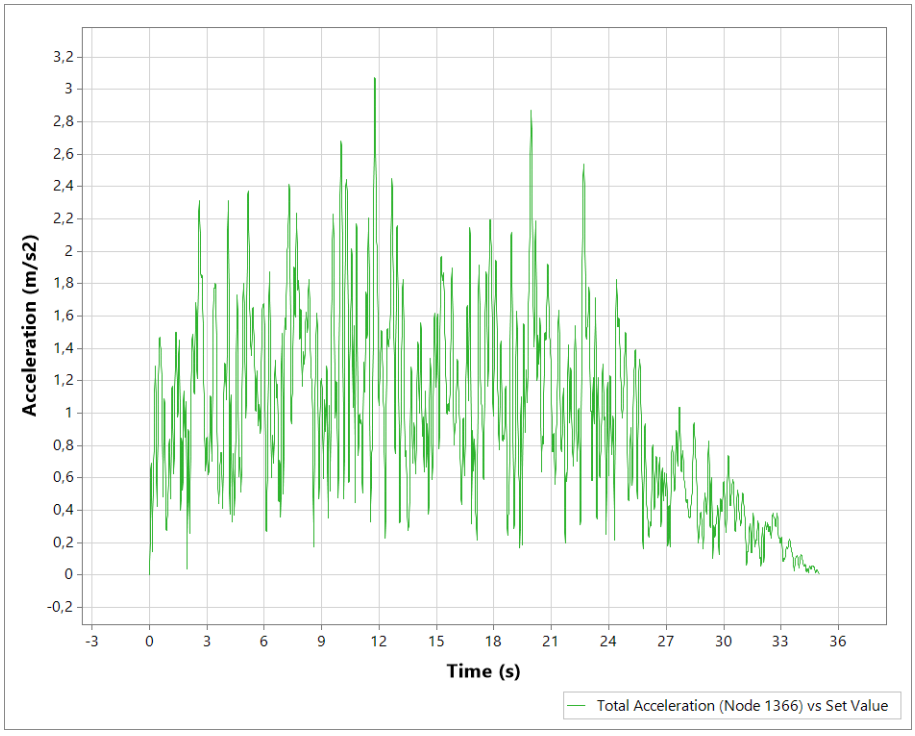

Fig. 29 *Total acceleration of the engine centre of gravity due to seismic load*

10. GENSET RESPONSE TO THE 2-PHASE SHORT CIRCUIT IMPULSE

The 2-phase short circuit appears if trunk wires, which are relatively close to the generator, are mutually connected. This causes an impulsive moment in the generator cross-section plane. The time history of the moment, given by the generator manufacturer, is shown in Figure 30. Its maximum value is *1.5 MNm*.

The impulsive moment is imposed on the FE model in the generator centre of gravity, Figure 8. It causes torsion of the base frame, as can be seen in Figure 31. Maximum von Mises stresses in the base frame occur in the area between the generator and the engine. Stress concentration reaches a value of *103 MPa*.

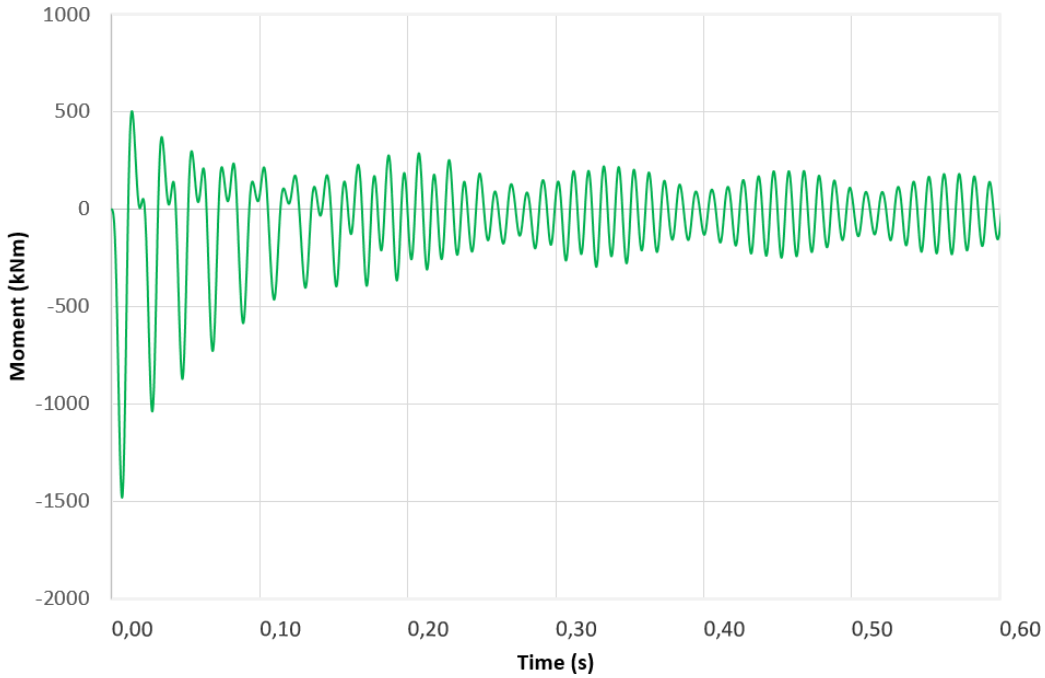

Fig. 30 *The 2-phase short circuit impulsive moment*

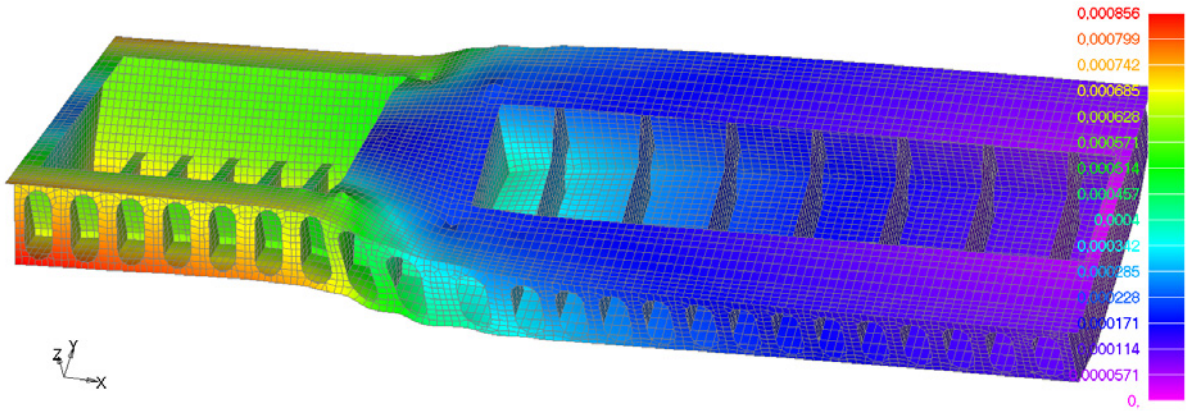

Fig. 31 *Deformation of the base frame due to the 2-phase short circuit moment, t = 0.012 s*

The maximum reaction forces taken from the corresponding time history diagrams are presented in Table 4. The maximum shear stresses in representative springs due to vertical and horizontal forces, determined by Eqs. (2) and (3), are listed in Table 5.

Table 4 *Maximum reaction forces due to the 2-phase short circuit (independent on time instant)*

Spring no.	*Node no.*	F_x *(kN)*	F_y *(kN)*	F_z*(kN)*	*F (kN)*
1	*9208*	*1.40*	*7.12*	*15.14*	*15.85*
2	*9215*	*1.25*	*7.10*	*15.02*	*15.85*
3	*9462*	*1.01*	*7.13*	*14.62*	*15.53*
4	*9519*	*0.89*	*7.08*	*8.97*	*10.43*
5	*9389*	*1.73*	*6.87*	*5.76*	*7.43*
6	*9216*	*2.14*	*6.16*	*6.07*	*7.65*
7	*9217*	*2.32*	*6.33*	*6.28*	*7.90*
8	*9213*	*2.40*	*7.31*	*6.42*	*8.69*
9	*9388*	*2.43*	*8.66*	*6.50*	*9.84*
10	*9209*	*2.45*	*10.00*	*6.55*	*11.05*
11	*1371*	*1.37*	*7.12*	*15.14*	*15.85*
12	*7905*	*1.25*	*7.10*	*15.02*	*15.85*
13	*8719*	*1.01*	*7.13*	*14.62*	*15.53*
14	*9157*	*0.89*	*7.08*	*8.97*	*10.43*
15	*8708*	*1.73*	*6.87*	*5.76*	*7.43*
16	*8018*	*2.14*	*6.16*	*6.07*	*7.65*
17	*8194*	*2.32*	*6.33*	*6.28*	*7.90*
18	*4077*	*2.40*	*7.31*	*6.42*	*8.69*
19	*8195*	*2.43*	*8.66*	*6.50*	*9.84*
20	*1373*	*2.45*	*10.00*	*6.55*	*11.05*

Table 5 *Maximum shear stresses in spring coils due to the 2-phase short circuit moment, τ (MPa)*

Spring No.	*Node No.*	τ_{F_z}	τ_{F_h}	τ_{tot}
1	*9208*	*37*	*21*	*58*
10	*9209*	*9*	*44*	*53*
11	*1371*	*37*	*21*	*58*
20	*1373*	*9*	*44*	*53*

11. GENSET RESPONSE TO SYNCHRONIZATION FAILURE LOAD

Synchronization failure of generator mostly happens when the synchronization device is suddenly out of order, or if it is not switched on in a proper time. This causes an impulsive moment in the generator cross-section plane. The moment time history is shown in Figure 32. It is characterized by a very short duration of only *0.6 s*, and a maximum amplitude of *1.35 MNm*.

The moment is imposed on the FE model in the generator centre of gravity, Figure 8. It causes torsion of the base frame, with a deformation shape very similar to that presented in Figure 31 in case of the 2-phase short circuit impulse. Maximum von Mises stresses in the base frame occur in the area between the generator and the engine with a magnitude of *135 MPa*.

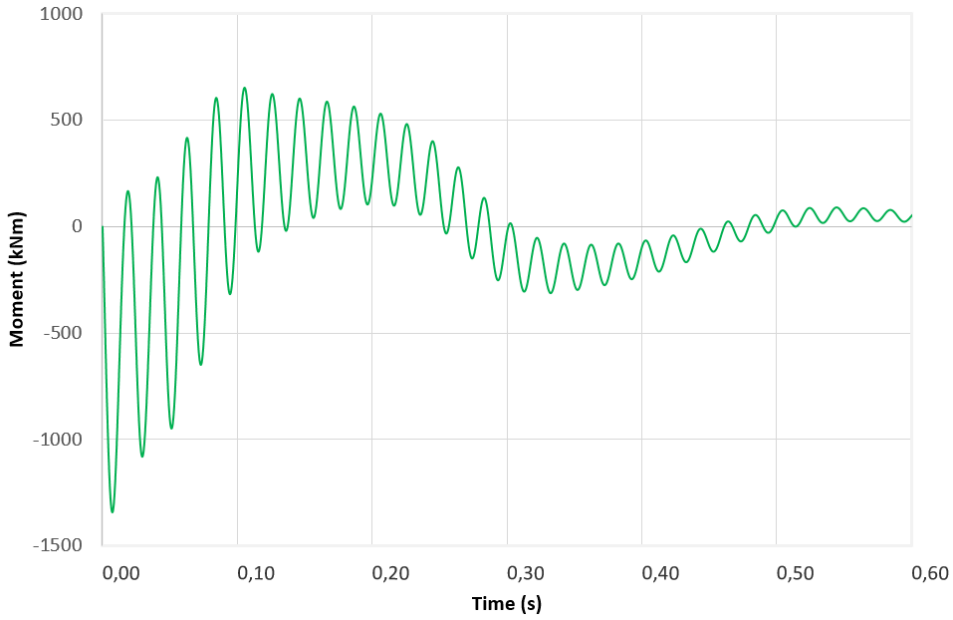

Fig. 32 *Synchronization failure impulsive moment*

The maximum values of spring reaction forces are listed in Table 6. The maximum shear stresses in representative springs, due to vertical and horizontal forces determined by Eqs. (2) and (3), are presented in Table 7. They are almost double the size compared to shear stresses in the case of the 2-phase short circuit impulse from Table 5.

Table 6 *Maximum reaction forces due to synchronisation failure (independent on time instant)*

Spring No.	*Node No.*	F_x *(kN)*	F_y *(kN)*	F_z *(kN)*	*F (kN)*
1	*9208*	*1.48*	*13.24*	*23.74*	*25.83*
2	*9215*	*1.40*	*13.03*	*23.57*	*25.75*
3	*9462*	*1.23*	*12.84*	*22.94*	*25.25*
4	*9519*	*1.35*	*12.60*	*15.80*	*18.55*
5	*9389*	*2.43*	*12.14*	*14.91*	*17.00*
6	*9216*	*2.86*	*11.15*	*14.95*	*17.23*
7	*9217*	*3.04*	*11.57*	*15.01*	*17.51*
8	*9213*	*3.11*	*13.43*	*15.04*	*17.85*
9	*9388*	*3.14*	*15.23*	*15.07*	*18.24*
10	*9209*	*3.16*	*17.01*	*15.09*	*18.93*
11	*1371*	*1.48*	*13.24*	*23.74*	*25.83*
12	*7905*	*1.40*	*13.03*	*23.57*	*25.75*
13	*8719*	*1.23*	*12.84*	*22.94*	*25.25*
14	*9157*	*1.35*	*12.60*	*15.80*	*18.55*
15	*8708*	*2.43*	*12.14*	*14.91*	*17.00*
16	*8018*	*2.86*	*11.15*	*14.95*	*17.23*
17	*8194*	*3.04*	*11.57*	*15.01*	*17.51*
18	*4077*	*3.11*	*13.43*	*15.04*	*17.85*
19	*8195*	*3.14*	*15.23*	*15.07*	*18.24*
20	*1373*	*3.16*	*17.01*	*15.09*	*18.93*

Table 7 *Maximum synchronisation failure shear stresses in spring coils, τ (MPa)*

Spring no.	***Node no.***	τ_{F_z}	τ_{F_h}	τ_{tot}
1	*9208*	*55*	*43*	*98*
10	*9209*	*17*	*73*	*90*
11	*1371*	*55*	*43*	*98*
20	*1373*	*17*	*73*	*90*

12. STRENGTH CRITERIA AND CAPACITY OF BASE FRAME

The base frame is a thin-walled structure made of ordinary-strength steel S235. Its physical characteristics are as follows, [8]:

Tensile strength: $R_m = 432.6$ *MPa*

Tensile stress at 0.2 elongation: $R_{0.2} = 243.4$ *MPa*

Yielding stress: $R_e = 236.2$ *MPa*

Stress proportionality limit: $R_p = 211.7$ *MPa*

Permissible stresses for the base frame are determined according to [9]. The design stress is defined as:

$$[\sigma] = min\left\{\frac{R_m}{n_m}; \frac{R_{0.2}}{n_{0.2}}\right\}, \tag{11}$$

where:

$n_m = 2.6$ for tensile strength,

$n_{0.2} = 1.5$ for stress at *0.2* elongation.

In the considered case:

$$[\sigma] = min\{166.4\ MPa; 162.3\ MPa\},$$

and value of $[\sigma] = 162.3$ *MPa* is relevant.

Permissible total (von Mises) membrane stress according to Table 5.1 in [10] reads:

$$[\sigma_s]_1 = 1.5 \cdot [\sigma] = 244\ MPa.$$

Permissible total membrane + bending (von Mises) stress takes value:

$$[\sigma_s]_2 = 1.9 \cdot [\sigma] = 308\ MPa.$$

Maximum von Mises total (membrane + bending) stresses in the base frame for different loading conditions are listed in Table 8. Membrane stresses in total von Mises membrane + bending stresses are predominant. Therefore, the criterion for permissible membrane stress of *244 MPa* is used. As reported in Sections 7 and 9, maximum stresses in the base frame due to gravity and seismic loads are induced above the elastic springs. Their sum reads *125 MPa* and is approximately *50 %* of the permissible stress.

Table 8 *Maximum von Mises total stresses, σ (MPa)*

Bottom		***Top***	
Gravity loads	***Seismic loads***	***2-phase short circuit***	***Synchronisation failure***
40.46	*84.23*	*102.17*	*132.29*

Maximum stresses due to the 2-phase short circuit impulse and synchronization failure load occur in the upper part of the base frame, where static stresses are negligible. Also, these two impulsive loads do not occur simultaneously. Each of the resulting maximum stresses meets the permitted stress criterion.

13. STRENGTH CRITERIA AND NUMBER OF SPRING-DAMPER ELEMENTS

Dimensions of the spring coils, the material used and characteristic strength values are not available from the manufacturer. Dimensions of coils are beforehand estimated in Section 4.

Springs are exposed to shear stresses due to vertical and horizontal forces, Eqs. (2) and (3). The limit shear stress can be defined as stress value due to vertical force, which causes maximum possible spring depression equal to the estimated clearances between coils, $\delta_c = 76$ *mm*. Hence, the limit force is $F_l = k_z \cdot \delta_c = 356$ *kN*, and the limit shear stress, according to Eq. (2), reads $\tau_l = 800$ *MPa*.

According to the spring element manufacturer, the maximum allowed spring deflection is $\delta_{al} = 47$ *mm*, while in operation it should not exceed $\delta_{op} = 43$ *mm*. Based on the above data one can write for the permissible shear stress in extreme cases:

$$\tau_{per} = \frac{\delta_{al}}{\delta_c}\tau_l = 495 \text{ MPa}$$

Static and dynamic analysis of the genset is performed by incorporating nominal $n_0 = 20$ spring elements in the FE model. The necessary number of springs can be determined proportionally to the actual shear stress due to different load combinations as:

$$n = \frac{\tau_{act}}{\tau_{per}} n_0 . \tag{12}$$

The maximum shear stress due to gravity load is determined in Section 7, while the maximum shear stresses for particular loads are listed in Tables 3, 5 and 7, respectively. The values are presented in Table 9. In the considered case, engine excitation forces are negligible, and corresponding shear stresses are ignored.

Table 9 *Maximum shear stresses in spring-damper elements due to particular loads, τ (MPa)*

Gravity load	***Seismic load***	***2-phase short circuit***	***Synchronisation failure***
177	*198*	*58*	*98*

The strength criteria for civil engineering structures and process components are given by the Russian Federal Codes and Standards in the Area of Atomic Energy Applications, [10]. The building of the emergency diesel electric power plant in the considered NPP is classified at the second seismic resistance category. For this category, the following load combinations in dynamic response analysis are required:

$$NO + DE, NOF + DE,$$

where NO is the normal operation, NOF is the normal operation with failure, while DE is the design earthquake.

The number of necessary spring-damper elements, determined for different loading combinations by Eq. (12), is shown in Table 10, as an even integer. Since the 2-phase short circuit can be caused by an earthquake, the necessary number of spring-damper elements to ensure the genset integrity is 18.

Table 10 *The necessary number of springs for different loading combinations*

Gravity load	***Gravity load and seismic load***	***Gravity load, seismic load and 2-phase short circuit***	***Gravity load, seismic load and synchronisation failure***
(7.15) *8*	*(15.15)* *16*	*(17.50)* *18*	*(19.11)* *20*

Strength criteria for helical springs exposed to shear stresses are not included in the Russian Federal Codes and Standards [10]. However, permissible tensional stresses are specified for bolts and studs, as well as for bearings, Tables 5.2 and 5.3 in [10], respectively. If these strength criteria are optionally used for helical springs, higher values of permissible stresses are obtained. This yields a smaller number of necessary spring elements and lower safety. Therefore, the guaranteed strength criteria provided by the spring manufacturer have to be used.

14. CONCLUSION

Dynamic analysis of the generator engine set is performed via the finite element method employing NASTRAN package. A simplified 3D FE model is generated. The base frame on elastic springs is modelled in detail by shell elements, while the generator and the engine are presented with lumped masses connected to the base frame with sets of massless bars.

The genset is located in the building of the emergency diesel electric power plant, which is classified as the second seismic resistance category. According to this fact, dynamic analyses of the genset are performed particularly for the seismic, the 2-phase short circuit, and the synchronisation failure loads.

Reaction forces and shear stresses in springs, due to vertical and horizontal forces, are determined for each load case. Satisfying required strength criteria given by the spring elements manufacturer, the necessary number of spring elements is determined for the possible load combinations. All springs are equipped with the damping device in order to effectively reduce the genset response. Since there is a possibility that an earthquake may cause the 2-phase short circuit, the necessary number of spring-damper elements is 18.

15. ACKNOWLEDGEMENT

This work has been supported by Croatian Science Foundation under the project IP-2019-04-5402.

16. REFERENCES

[1] O.C. Zienkiewicz, *The Finite Element Method in Engineering Science*, McGraw-Hill, London, 1971.

[2] S. Timoshenko, *Strength of Materials, Part 1, Elementary Theory and Problems*, 3rd edition, Krieger Pub Co, 1983.

[3] D. Čakmak, Z. Tomičević, H. Wolf, Ž. Božić, D. Semenski, On cylindrical coil spring deflection and stress: An analytical and numerical study (submitted)

[4] MSC Software, MD NASTRAN 2010 Dynamic analysis user's guide, MSC Software, 2010.

[5] R.W. Clough, J. Penzien, *Dynamics of Structures*, McGraw Hill, Inc., 1975.

[6] A. Mihanović, *Dinamika konstrukcija*, Građevinski fakultet, Split, 1995.

[7] M. Hrasnica, Spektri odgovora za seizmičku procjenu zgrada, Građevinar, Vol. 54, No. 11, pp. 657-663, 2002.

[8] DNV-RP-C208, Determination of Structural Capacity by Non-linear FE analysis Methods, June, 2013.

[9] Codes for strength analysis of nuclear power plant energetic components, PN AE G-7-002-86; Federal nuclear and radiation safety regulatory authority of Russia (Gosatomnadzor of Russia) 1986, (in Russian).

[10] Federal Codes and Standards in the Area of Atomic Energy Applications, Standards for Design of Seismic Resistant Nuclear Power Plant NP-031-01; Federal nuclear and radiation safety regulatory authority of Russia (Gosatomnadzor of Russia), 2002.